مجلة جامعة الزاوية للعلوم الطبيعية
University of Zawia Journal of Natural Sciences *(UZJNS)*
https://journals.zu.edu.ly/index.php/UZJNS ISSN: 3078-4999

Numerical Calculation of Attenuation Mechanisms in Single-Mode Optical Fibres

Nesrin A Alshatwi[a], Mariam O Madi[b*], Salma A Amhammed[a]

[a] *Department of Physics, Faculty of Science, University of Sirte, Sirte, Libya*

[b] *Department of Physics, Faculty of Science, University of Tripoli, Tripoli, Libya*

**Corresponding email author: ma.madi@uot.edu.ly*

Received 04 Jan 2026 | Accepted 30 Mar 2026 | Available online 31 Mar 2026 | DOI: 10.26629/uzjns.2026.03

A B S T R A C T

This study presents a numerical analysis of attenuation mechanisms in single-mode silica optical fibers. The wavelength-dependent behavior of Rayleigh scattering, intrinsic and extrinsic material absorption, ultraviolet and infrared absorption, and bending losses is systematically investigated. The results show that Rayleigh scattering dominates at shorter wavelengths and decreases rapidly with increasing wavelength, consistent with its inverse fourth-power ($1/\lambda^4$) dependence. Material absorption introduces pronounced loss peaks associated with hydroxyl (OH^-) impurities, particularly near 1380 nm, which significantly limits transmission in this region. Infrared absorption increases at longer wavelengths due to vibrational modes of the silica lattice, while ultraviolet absorption decreases with wavelength and contributes negligibly within standard communication bands. Bending losses exhibit strong dependence on both bending radius and wavelength, with higher attenuation observed at smaller bend diameters and longer wavelengths. The combined attenuation profile reveals a minimum-loss transmission window in the 1300–1550 nm range, confirming its suitability for optical communication systems.

Keywords: *Fiber optics, Rayleigh scattering, absorption, bending loss, loss coefficient.*

الحساب العددي لآليات التوهين في الألياف الضوئية أحادية النمط

نسرين عبد الجليل الشتيوي[a] ، مريم عمران مادي[b] ، وسالمة احميد امحمد[a]

[a] قسم الفيزياء، كلية العلوم، جامعة سرت، سرت، ليبيا

[b] قسم الفيزياء، كلية العلوم، جامعة طرابلس، طرابلس، ليبيا

الملخص

تقدم هذه الدراسة تحليلاً عددياً لآليات التوهين في الألياف الضوئية أحادية النمط المصنوعة من السيليكا. وتدرس سلوك تشتت رايلي، وامتصاص المادة الداخلي والخارجي، وامتصاص الأشعة فوق البنفسجية والأشعة تحت الحمراء، وفقدان الانحناء، تبعاً لتغير الطول الموجي. وتُظهر النتائج أن تشتت رايلي هو السائد عند الأطوال الموجية القصيرة، ويتناقص بسرعة مع زيادة الطول الموجي، بما يتوافق مع اعتماده العكسي على القوة الرابعة ($1/\lambda^4$). ويُسبب امتصاص المادة ذروات فقدان واضحة مرتبطة بشوائب الهيدروكسيل (OH^-)، خاصة بالقرب من **1380nm**، مما يحد بشكل كبير من النقل في هذه المنطقة. ويزداد امتصاص الأشعة تحت الحمراء عند الأطوال الموجية الأطول نتيجة لأنماط اهتزاز شبكة السيليكا، بينما يتناقص امتصاص الأشعة فوق البنفسجية مع زيادة الطول الموجي، ويصبح تأثيره ضئيلاً ضمن نطاقات الاتصالات القياسية. تظهر خسائر الانحناء اعتماداً كبيراً على كلٍ من نصف قطر الانحناء والطول الموجي، حيث يُلاحظ توهين أعلى عند أقطار الانحناء الأصغر والأطوال الموجية الأطول. ويكشف منحنى التوهين المُجمّع عن نافذة نقل ذات أدنى خسارة في نطاق **1300-1550 nm**، مما يؤكد ملائمتها لأنظمة الاتصالات الضوئية.

الكلمات المفتاحية: *الألياف البصرية، تشتت رايلي، الامتصاص، فقدان الانحناء، معامل الفقد.*

1. Introduction

Optical fiber communication plays a pivotal role in the development of high-quality, high-speed telecommunication systems. In addition to telecommunication links, optical fibers are extensively utilized in the Internet and Local Area Networks (LAN) to achieve high signalling rates [1], [2], [3].

Optical fibers are generally classified as either single-mode or multimode, depending on their electromagnetic propagation characteristics. Single-mode fibers (SMFs) are distinguished by a significantly reduced core diameter—typically ranging from 8 to 10 µm—which ensures the propagation of only a single spatial mode, effectively eliminating modal dispersion. Due to this characteristic, SMFs are the preferred choice for long-haul transmission and high-fidelity applications where signal integrity and low attenuation are paramount. Furthermore, their precision makes them indispensable in advanced medical diagnostics, including endoscopy and Optical Coherence Tomography (OCT), to achieve superior imaging resolution [4].

Multimode fibers (MMFs) are characterized by a substantially larger core diameter, typically ranging from 50 to 100 µm. This structural design facilitates more efficient light coupling from various sources, enables the transmission of higher optical power, and permits the simultaneous propagation of multiple spatial modes. Consequently, MMFs are ideal for applications requiring high light intensity or expanded beam diameters over relatively short distances. Such properties make them particularly effective in specialized medical fields, including photodynamic therapy and laser surgery [5], [6]. Furthermore, multimode fibers significantly enhance sensing capabilities by enabling multiplexed signal detection and the parallel analysis of diverse samples. This inherent capacity for spatial multiplexing facilitates accelerated data acquisition and substantially increases system throughput. Such advantages make MMFs an instrumental component in high-efficiency sensing applications where rapid, multi-channel processing is essential [7], [8]. Despite their advantages, optical fiber communication systems encounter various attenuation mechanisms that inherently degrade overall system performance [9].

This paper aims to systematically analyze the diverse loss phenomena within single-mode fibers (SMFs) and investigate strategies for their mitigation by employing a MATLAB program. This study evaluates these mechanisms to optimize transmission efficiency in optical fiber communication networks.

2. Theory Part

Attenuation in optical fibers is inherently wavelength-dependent, dictated by the physical properties of the transmission medium. In the telecommunications industry, the wavelength range of 1430–1580 nm is strategically utilized, as it aligns with the operational gain bandwidth of optical fiber amplifiers. This spectral region ensures efficient signal amplification and minimal loss over long-distance transmission [10]. Attenuation represents the loss of optical power as light propagates through the fiber medium. It is quantitatively defined as the ratio between the input power (p_{in}), launched from the source, and the output power (p_{out}), measured at the receiver end [11]. This parameter is critical in determining the maximum transmission distance before signal regeneration becomes necessary. The attenuation coefficient per unit length, typically expressed in decibels per kilometer (dB/km), is defined by the following relation [9], [12]:

$$\alpha_{dB} = \frac{10}{L}\log_{10}\left(\frac{p_{in}}{p_{out}}\right) \quad (1)$$

Signal attenuation is expressed through a logarithmic relationship per unit length, typically measured in decibels per kilometer (dB/km). For a fiber of length (L) (expressed in kilometers), this loss is a fundamental parameter in system design [11], [13]. Attenuation is a critical parameter in the design of global telecommunication systems, and it is particularly fundamental in optical fiber network engineering. The degradation of the optical signal occurs due to various physical phenomena encountered along the transmission links. Specifically, as light propagates through the fiber, it suffers from intrinsic losses dictated by the chemical composition and the molecular structure of the silica material. These losses are primarily governed by the interaction between photons and the fiber's internal medium, which includes both absorption and scattering mechanisms [14].

Furthermore, attenuation mechanisms such as scattering and macro-bending losses arise from the granular and geometric characteristics of the optical fiber. The presence of metallic ions and hydroxyl OH^{-1} impurities significantly contributes to light scattering and absorption. It is essential to emphasize

that the balance between absorption and scattering is intrinsically linked to the operating wavelength, as well as the specific chemical composition of the silica glass [15], [16].

The attenuation in optical fibers is primarily governed by impurities within the silica-based medium. While photon absorption in the infrared spectrum leads to increased losses at shorter wavelengths, standard low-loss fibers exhibit an optimal minimum attenuation of approximately (0.1 dB/km) at (1.55µm band), this loss profile is a composite of various factors, including material absorption, scattering, mode coupling, and macro/micro-bending, as well as structural defects and radiation-induced attenuation [17].

Generally, these phenomena are categorized into three fundamental mechanisms: Scattering, Absorption and Bending.

2.1. Scattering Losses

In optical fibers, scattering losses originate from microscopic variations in material density, compositional fluctuations, and structural inhomogeneities or defects introduced during the fabrication process. At the molecular level, glass is characterized by a randomly distributed network of molecules [16].

The amorphous nature of glass inherently leads to localized fluctuations where the molecular density deviates—either higher or lower—from the material's average density. Furthermore, since optical glass is typically synthesized from a combination of multiple oxides, including SiO_2, GeO_2, and P_2O_5, stochastic compositional fluctuations are inevitable. These dual phenomena induce microscopic refractive-index variations on a spatial scale significantly smaller than the operating wavelength [18]. The primary origin of scattering loss is fundamentally linked to the relationship between the attenuation levels and the specific geometrical and physical parameters of the waveguide. This loss is often a direct consequence of structural imperfections inherent in real photonic waveguides [19]. In general, scattering mechanisms in optical fibers can be categorized into two main types.

2.1.1. Rayleigh Scattering

The leading cause of intrinsic optical attenuation in silica fibers is Rayleigh scattering [20]. Rayleigh scattering is caused by light reflecting off of molecules in the glass whose diameter is 1/10 the wavelength of the light [21]. Rayleigh scattering arises from the inherent inhomogeneities within the optical fiber medium. Specifically, the stochastic arrangement of molecules leads to localized density variations, which in turn cause fluctuations in the refractive index [22]. As an elastic scattering process, the frequency of the scattered light remains identical to that of the incident light [23]. This phenomenon is the decisive factor in determining transmission loss, resulting from density fluctuations that become 'frozen' into the fused silica during fabrication, creating refractive index gradients along the fiber length [24]. The intrinsic loss coefficient of the optical fiber due to Rayleigh scattering is mathematically defined as [11]:

$$\alpha_R = \frac{A}{\lambda^4} \qquad (2)$$

The Rayleigh scattering coefficient A depends on the glass composition and temperature during fabrication. A in pure silica $\approx 0.7 - 0.9(dB.K^{-1}.\mu m^{-4})$ [25].

The scattering coefficient A is theoretically related to the microscopic fluctuations in refractive index by the following expression [26]:

$$A = (8\,\pi^3\,n^8\,p^2\,\beta_T\,k_B\,T/3) \qquad (3)$$

Where: n is the refractive index of the fiber core, p is photo elastic coefficient of silica, β_T is the isothermal compressibility, k_B is the Boltzmann constant, and T is the absolute temperature.

This relation shows that Rayleigh scattering increases with temperature and refractive index, and decreases sharply with the fourth power of wavelength (λ^{-4}), explaining why longer wavelengths (e.g., 1550 nm) exhibit lower attenuation. In this spectral region, Rayleigh scattering constitutes the primary source of intrinsic loss. This dominance facilitates the estimation of total fiber attenuation through the characterization of Rayleigh backscattering (RBS) power levels. Consequently, the longitudinal distribution of optical power follows an exponential decay model relative to the propagation distance L, as defined by the following equation [9]:

$$p_{out}(L) = p_{in}e^{-\alpha L} \qquad (4)$$

$$p_{out}(L) = p_{in}10^{-(\alpha_{dB}L/10)} \qquad (5)$$

2.1.2. Mie Scattering

Linear scattering also arises from structural inhomogeneities with dimensions comparable to the guided wavelength [27], [28]. These phenomena are primarily attributed to deviations from the ideal cylindrical geometry of the waveguide. Specifically, imperfections such as core–cladding interface irregularities, longitudinal variations in the refractive index profile, diameter fluctuations, and

the presence of localized strains or bubbles contribute to this loss mechanism [29], [30].

When the dimensions of scattering inhomogeneities approach or exceed the threshold of λ/10, the system undergoes a transition from the Rayleigh regime to the Mie or geometric scattering regimes. In this state, the angular dependence of the scattered intensity becomes increasingly pronounced, and the total scattering cross-section may rise substantially [31].

Mie scattering, which arises from these specific inhomogeneities, is characterized by a predominantly forward-directed radiation pattern. Unlike the more isotropic distribution seen in Rayleigh scattering, this phenomenon concentrates the scattered energy along the primary axis of propagation [32]. The magnitude of Mie scattering-induced attenuation is contingent upon the fiber's material composition, geometric design, and fabrication precision. Strategic reduction of these losses can be achieved through

(a) removing imperfections due to the glass manufacturing process.

(b) carefully controlled extrusion and coating of the fiber.

(c) increasing the fiber guidance by increasing the relative refractive index difference.

By these means, it is possible to reduce Mie scattering to insignificant levels [33],[34].

2.2. Material Absorption Loss

Material absorption is a loss mechanism related to the material composition and the fabrication process for the fiber, which results in the dissipation of some of the transmitted optical power as heat in the waveguide. The absorption of the light may be intrinsic (caused by the interaction with one or more of the major components of the glass) or extrinsic (caused by impurities within the glass) [35].

2.2.1. Extrinsic Attenuation

Extrinsic attenuation is primarily attributed to the presence of interstitial impurity atoms introduced during the glass synthesis phase. These contaminants, predominantly transition metal ions, even at concentrations as low as parts per billion (ppb) and hydroxyl (OH^-) radicals, introduce specific electronic and vibrational absorption peaks. Notably, the (OH^-) ions manifest as distinct absorption bands at approximately 950 nm, 725 nm, and 2700 nm, creating the well-known 'water peaks' that constrain the fiber's operational bandwidth. [36].

The intrinsic variability and non-uniform distribution of structural defects in silica fibers preclude the derivation of a universal analytical model for absorption. Instead, extrinsic losses are typically characterized via a phenomenological approach, wherein the total absorption profile is modelled as a superposition of discrete Gaussian bands. Each Gaussian component represents the localized energetic contribution of a specific defect centre within the glass matrix, as defined by the following equation:

$$\alpha_{def} = A_i e^{\left(-\frac{(\lambda-\lambda_i)^2}{2\sigma_i^2}\right)} \quad (6)$$

Where α_{def} Defect-related absorption coefficient at wavelength λ, A_i Peak absorption amplitude associated with the *i-th defect centre* with values of 0.5, 0.6, and 0.7 dB/km, respectively.

λ_i defines the centre wavelength of the Gaussian absorption band associated with a specific defect or impurity, λi of the Gaussian peaks are chosen to correspond to the experimentally observed absorption bands at approximately 950 nm, 1240 nm, and 1380 nm.

σ_i is the standard deviation of the Gaussian function, which determines the spectral width of the absorption band, reflecting the extent of wavelength broadening caused by the defect distribution within the material, was selected in the range of 30–50 nm.

2.2.2. Intrinsic Absorption:

It is dictated by the fundamental atomic constituents of the glass matrix and establishes the ultimate lower limit for fiber attenuation [18]. This limit is defined by two physical phenomena: electronic transitions within the ultraviolet (UV) spectrum and molecular bond vibrations in the infrared (IR) region [37]. Consistent with established empirical models for silica-based media, the UV absorption edge is characterized by an exponential decay, whereas the IR tail exhibits exponential growth.

The convergence of these mechanisms creates a distinct minimum-loss transmission window in the visible-to-near-infrared range, a hallmark of high-purity SiO_2 waveguides [38]. The equation used to calculate α_{IR} is given by [25], [39]:

$$\alpha_{IR} = Ce^{-c/\lambda} \quad (7)$$

In the numerical model, the constants C and c serve as empirical fitting parameters, the values C=5.4 $dB.Km^{-1}$ and c=7840nm are adopted to represent the infrared absorption behavior of high-purity SiO_2 fibers. These values are iteratively refined to ensure high fidelity between the numerical model and the experimentally measured infrared absorption profiles characteristic of silica-based optical fibers. The equation used to calculate the α_{UV}, is given by:

$$\alpha_{UV} = A_{UV} e^{\frac{4.63}{\lambda}} \quad (8)$$

Where: A_{UV} is an empirical constant (material-dependent), A_{UV} In pure silica is $0.0261\ dB.Km^{-1}$[39].

2.3. Bending Loss

Bending loss in optical fibers occurs due to structural deformations, which alter the refractive index and angle of incidence of light within the fiber core. Bending effects are generally classified into [40].

2.3.1 Macro Bending Loss

Macro bending losses are triggered when a fiber is subjected to large-radius curvature, resulting in the radiation of light into the cladding. These losses often stem from unintentional physical displacements that alter the light's propagation path. As the fiber curves, the light rays deviate from the core's axis, failing to maintain total internal reflection and instead escaping into the cladding layer [40], [41].

2.3.2 Micro Bending Loss

Losses arise from microscopic structural imperfections at the core-cladding interface. These defects typically result from manufacturing flaws, improper cabling processes, thermal contraction at low temperatures, or localized mechanical stress. Unlike macro bending, micro bending is significantly harder to detect because the bend radii are comparable to the fiber's core radius, leading to intermodal power coupling. These losses can be mitigated by applying a flexible protective jacket to the fiber [37], [40], [42], [43]. When a fiber is bent, the plane wave fronts associated with the guided mode are pivoted at the centre of curvature and their longitudinal. Velocity along the fiber axis. Increases with the distance from the centre of curvature. As the fiber is bent further. Over a critical curve, the phase velocity exceeds that of the plane wave in the cladding. And radiation occurs [44]. The bending-induced attenuation α_B in the single-mode optical fiber was evaluated using the analytical model developed by Marcuse. The bend loss α_B for a radius of curvature R is given by:

$$\alpha_B = c\frac{1}{\sqrt{R}} e^{\left(\frac{-2R\Delta}{a}\frac{V^2}{u^2}\right)} \quad (9)$$

$$V = \frac{2\pi a}{\lambda}\sqrt{{n_1}^2 - {n_2}^2} \quad (10)$$

$$\Delta = \frac{({n_1}^2 - {n_2}^2)^{3/2}}{{n_2}^2} \quad (11)$$

Where: C is a normalization factor adjusted according to fiber specifications, its approximation as 1×10^3R is the radius of curvature of the fiber bend, λ is the wavelength, a is the core radius of the optical fiber, u is the first zero of the Bessel function for the fundamental mode, which is approximated as u≈2.405. n_1 is the refractive index of the fiber core and n_2 is the refractive index of the cladding [45]. Table 1 shows the relevant single-mode optical fiber characteristics [46].

Table 1: Main characteristics of the silica optical fiber.

Optical fiber	Silica
Radius of curvature	15×10^{-3}m
Refractive index of the core	1.450
Refractive index of the cladding	1.445
Core radius	6×10^{-6} m

2.4. Total Loss

Rayleigh scattering, material absorption and Bending are three mechanisms for the fiber loss. The total attenuation coefficient is denoted as α (with the units of dB.km[1]). In the wavelength of 1550 nm, which is commonly used in optical communication, the attenuation coefficient is about 0.2 dB/km in the standard single-mode fiber (SMF) [47]. Considering the scattering coefficient in the range 0.12-0.16 dB/km, the total loss can be expressed as a sum of the contributions:

$$\alpha_{tot} = \alpha_R + \alpha_{IR} + \alpha_{def} + \alpha_{UV} + \alpha_B \quad (12)$$

3. Results and Discussion

This section presents the calculated attenuation coefficients for the optical fiber. Total attenuation is the result of several physical mechanisms, primarily material absorption, bending losses (including microbending), and scattering losses. Among these, Rayleigh scattering is a dominant factor. Figure 1 illustrates the variation of Rayleigh scattering loss as a function of wavelength, covering a range up to 1700 nm for a single-mode optical fiber. As demonstrated by Eq. (2), Rayleigh scattering exhibits a strong inverse dependence on wavelength. The results show higher attenuation at shorter wavelengths, which significantly decreases as the wavelength increases. Specifically, the loss is approximately 2.7 dB/km at 800 nm, dropping gradually to below 0.2 dB/km near 1600 nm. This trend aligns with the theoretical ($1/\lambda^4$) relationship, where shorter wavelengths interact more intensely with microscopic inhomogeneities in the fiber material. Conversely, longer wavelengths, particularly within the 1300 nm and 1550 nm

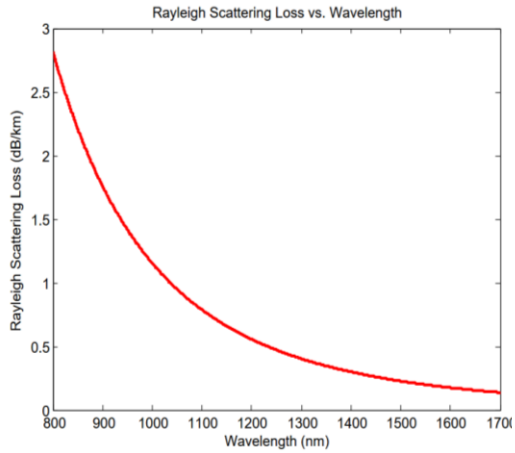

Figure 1 Calculated Rayleigh scattering loss as a function of wavelength (nm) for a single-mode silica fiber.

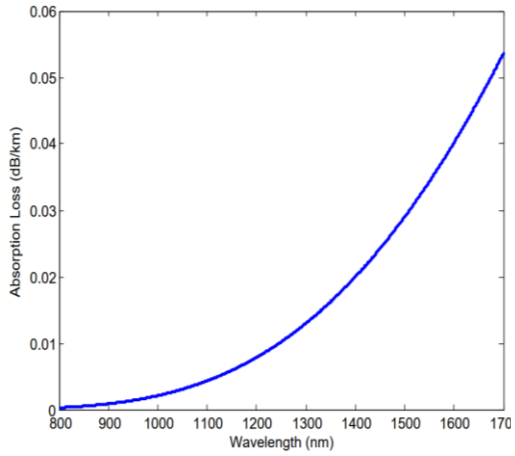

Figure 2 Intrinsic infrared (IR) absorption loss in a single-mode silica fiber as a function of wavelength (800–1700 nm).

telecommunication windows, experience minimal scattering. This makes these regions ideal for long-distance transmission. Overall, these findings highlight the critical role of Rayleigh scattering in defining the operational windows of modern optical systems and are in excellent agreement with established literature, e.g. [48].

Figure 2 illustrates the intrinsic infrared (IR) absorption loss in silica optical fibers was computed using an exponential decay model across a wavelength range of 800 nm to 1700 nm. As indicated by Eq. (7), the results demonstrate a clear monotonic increase in absorption loss as the wavelength shifts toward the infrared region. At shorter wavelengths, specifically those below approximately 1000 nm, the contribution of IR absorption remains negligible. However, beyond 1200 nm, the loss coefficient rises at an accelerating rate. This trend reflects the increasing influence of intrinsic vibrational absorption mechanisms (multiphonon absorption) inherent in the molecular structure of silica glass. These results are largely consistent with theoretical expectations and are in excellent agreement with established literature, such as the work of [48] and [49].

Figure 3 shows the variation of material absorption loss in an optical fiber as a function of wavelength. Unlike Rayleigh scattering loss, which decreases monotonically with wavelength, absorption loss exhibits distinct peaks corresponding to specific absorption bands. These peaks are mainly attributed to residual impurities in the glass material, particularly hydroxyl (OH^-) ions, as well as vibrational overtones of the silica lattice. As observed from Eq. (6), a moderate absorption peak appears near 950 nm, followed by a broader and more pronounced absorption band between 1200 nm and 1400 nm, reaching its maximum of approximately 1.2 dB/km around 1380 nm. This strong absorption is associated with the fundamental vibrational modes of OH^- related impurities, which significantly degrade transmission performance in this spectral region. Another smaller absorption feature can also be observed near 1240 nm, which is linked to higher-order vibrational harmonics. These absorption characteristics are crucial in defining the transmission "windows" of optical fibers. Specifically, the strong absorption around 1380 nm creates a "forbidden region" that limits efficient transmission in this range. Consequently, modern communication systems are designed to operate within low-loss windows around 1310 nm and 1550 nm, where the absorption is minimal. In summary, Figure 3 emphasizes the importance of material purity and advanced fabrication techniques in minimizing absorption losses, thereby enabling ultra-low-loss optical fibers suitable for long-haul telecommunication applications. The results obtained are found to be in good agreement with that found in the literatures, such as reference [35].

Figure 4 shows the ultraviolet absorption coefficient as a function of wavelength over a wide spectral range extending from the near-visible to the near-infrared region.

As observed from Eq. (8), the variation of the

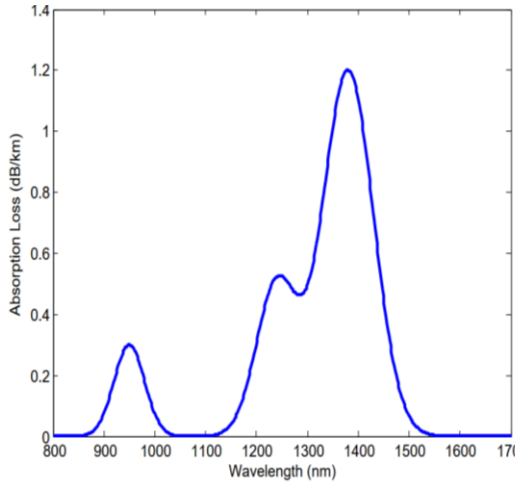

Figure 3 Material absorption loss in optical fiber as a function of wavelength.

ultraviolet absorption coefficient with wavelength is in the range from 700 nm to 1800 nm. A gradual decrease in the absorption coefficient is observed as the wavelength increases, which is consistent with the reduced contribution of high-energy electronic transitions responsible for ultraviolet absorption. This behaviour indicates that ultraviolet absorption becomes less significant at longer wavelengths, contributing minimally to the total attenuation in the typical operating wavelength range of optical communication systems. These results are in good agreement with the results found in the literatures e.g. [1].

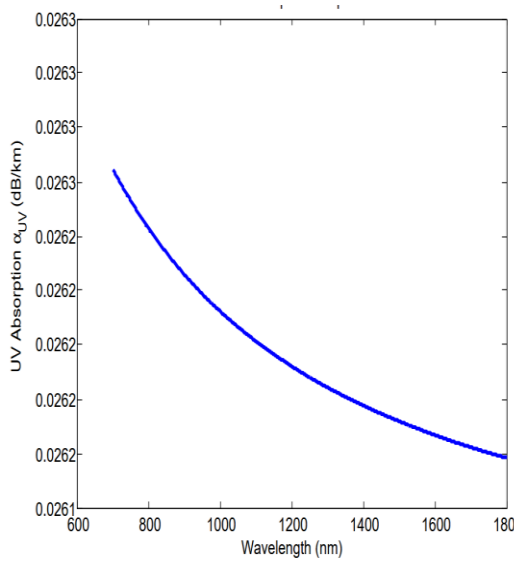

Figure 4 Ultraviolet absorption coefficient as a function of wavelength in optical fiber.

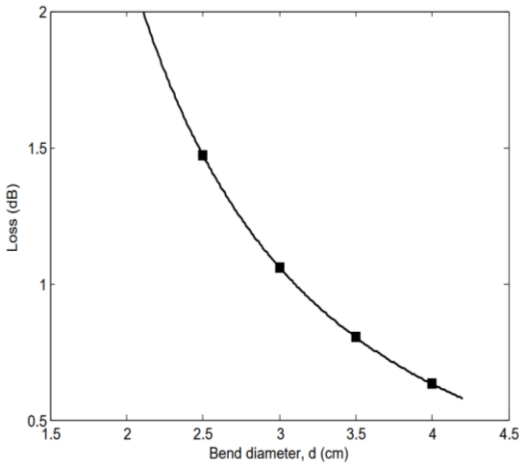

Figure 5 Calculated macro bending loss as a function of bend diameter in a single-mode fiber.

Figure 5 gives the impact of the bend diameter on optical attenuation. As demonstrated by the calculations in Eq. (9), there is a clear and consistent trend: optical loss decreases progressively as the bend diameter increases. The results indicate that bending loss is significantly higher at smaller diameters. This is due to the sharp curvature of the fiber, which weakens mode confinement and triggers substantial radiation leakage into the cladding. As the bending radius is increased, the curvature becomes less severe, allowing the guided mode to remain more effectively confined within the core, thereby resulting in a gradual reduction in attenuation. This smooth, monotonic decrease emphasizes the high sensitivity of single-mode fibers to macro bending effects, particularly when the bend diameter falls below 3cm. These findings demonstrate that maintaining a minimum bend radius is critical for minimizing signal degradation in fiber installations. The results obtained are in close agreement with theoretical models, for example [42], [50].

Figure 6 depicts the spectral dependence of bending loss for a single-mode optical fiber, as determined by the Marcuse theoretical formulation outlined in Eq. (9). This analysis shows that as the operating wavelength rises from 800 nm to 1700 nm.

The results reveal a pronounced increase in bending loss with increasing wavelength, indicating that optical fibers become considerably more susceptible to bending effects at longer wavelengths. This behavior is primarily attributed to the reduction in optical mode confinement as the wavelength increases, which enhances radiation leakage from the fiber core under bending conditions.

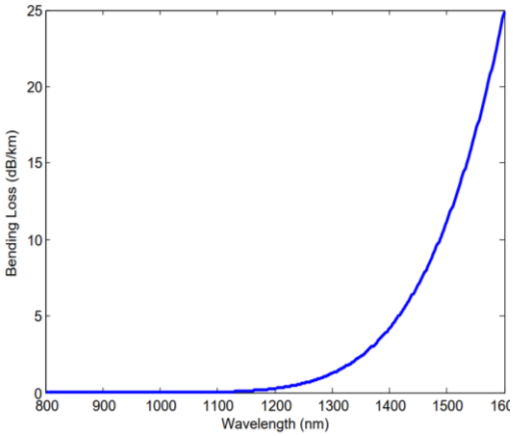

Figure 6 Calculated bending loss as a function of wavelength (800–1700 nm) for a single-mode fiber, based on the Marcuse model (Eq. 9).

Consequently, the bending-induced attenuation exhibits a sharp rise, reflecting the exponential sensitivity of fiber losses to curvature at longer wavelengths. This phenomenon can be physically explained by the enlargement of the mode field diameter and the weakened confinement of the guided mode, leading to increased radiation loss when the fiber is bent.

The obtained results are consistent with classical waveguide theory and demonstrate that operation at shorter wavelengths significantly improves bend tolerance in optical fiber systems. Moreover, the present findings show good agreement with previously reported results in the literature, such as those presented by [51].

Figure 7 illustrates the wavelength dependence of attenuation in silica optical fibers by presenting the individual contributions of the dominant loss mechanisms along with their combined effect, as calculated using Eq. (12).

At short wavelengths (below ~900 nm), the total attenuation is dominated by Rayleigh scattering, which decreases rapidly with increasing wavelength. due to its inverse power-law dependence. As the wavelength increases toward the near-infrared region, Rayleigh scattering becomes less significant, leading to a general reduction in total loss. Distinct absorption features are observed due to hydroxyl (OH^-) impurities, appearing as localized peaks around specific wavelengths (notably near ~950 nm and ~1240 nm). These peaks indicate the strong influence of residual OH^- ions even at low concentrations, causing noticeable increases in attenuation at those wavelengths. In the longer wavelength region (>1400 nm), infrared absorption rises sharply and becomes the dominant loss

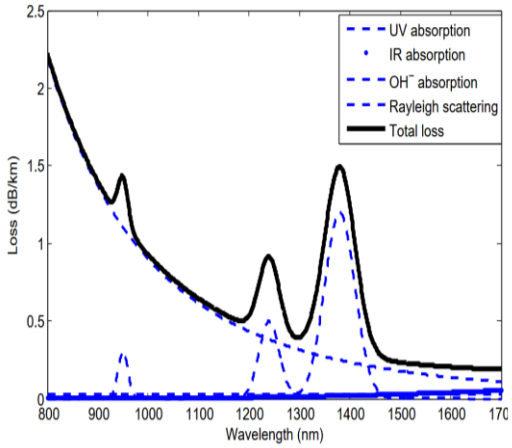

Figure 7 Total spectral attenuation in a single-mode silica fiber, showing the combined effects of Rayleigh scattering, hydroxyl (OH^-) absorption, and the infrared absorption tail.

mechanism, resulting in a pronounced increase in total attenuation.

The superposition of all mechanisms produces a minimum attenuation window in the range of approximately 1300–1550 nm, which explains why these wavelengths are widely used in optical fiber communication systems. Overall, the figure clearly demonstrates how different physical mechanisms govern fiber attenuation across the spectrum and highlights the importance of material purity and wavelength selection in minimizing transmission losses.

4. Conclusion

This work conducted an in-depth examination of the attenuation mechanisms present in single-mode silica optical fibers. Our results show that Rayleigh scattering dominates at shorter wavelengths and decreases rapidly with increasing wavelength, while material absorption introduces distinct loss peaks associated with OH^- impurities and intrinsic vibrational modes of silica. Ultraviolet absorption was found to decrease with wavelength and contributes negligibly within the standard communication bands.

Bending losses exhibit strong dependence on both bending radius and operating wavelength, with higher attenuation occurring at smaller bend diameters and longer wavelengths due to reduced mode confinement. The combined attenuation analysis confirms a minimum-loss transmission window in the range of 1300–1550 nm, validating its suitability for modern optical communication systems. The results that are shown in this work have excellent agreement with theoretical models and

existing literature, offering practical insights for the optimization of fiber design and deployment.

References

[1] M. Arumugam, “Optical fiber communication—An overview,” *Pramana*, vol. 57, no. 5, pp. 849-869, 2001.

[2] A. N. Z. Rashed, “Optical fibre communication cables systems performance under harmful gamma irradiation and thermal environment effects,” *IET Communications*, vol. 7, no. 5, pp. 448-455, 2013.

[3] P. Sharma, R. K. Arora, S. Pardeshi, and M. Singh, “Fibre optic communications: An overview,” *International Journal of Emerging Technology and Advanced Engineering*, vol. 3, no. 5, pp. 474-479, 2013.

[4] E.-G. Neumann, *Single-mode fibers: fundamentals*: Springer, 2013.

[5] B. Huang, “Mode Evolution in Fiber Based Devices for Optical Communication Systems,” M.S. thesis, University of Central Florida, Florida, 2017.

[6] O. Korichi, M. Hiekkamäki, and R. Fickler, “High-efficiency interface between multi-mode and single-mode fibers,” *Optics Letters*, vol. 48, no. 4, pp. 1000-1003, 2023.

[7] Y. Hu, P. Minzioni, J. Hui, S. H. Yun, and A. K. Yetisen, “Fiber optic devices for diagnostics and therapy in photomedicine,” *Advanced Optical Materials*, vol. 12, no. 22, pp. 2400478, 2024.

[8] A. Abdelali, “Analysis and Modelling of High-Speed Optical Fiber Transmission System,” M.S. thesis, University of Faculté des sciences et de la technologie, 2025.

[9] M. N. Uddin, D. M. M. Rahman, and M. S. Ali, “Performance analysis of different loss mechanisms in optical fiber communication,” *Computer Applications: An International Journal (CAIJ)*, vol. 2, no. 2, pp. 1-13, 2015.

[10] S. H. Saeid, "Computer simulation and performance evaluation of single mode fiber optics," *Proceedings of the World Congress on Engineering*, vol. II, London, U.K., Jul. 4–6, pp. 1007–1012, 2012.

[11] X. Bao, and Y. Wang, “Recent advancements in Rayleigh scattering-based distributed fiber sensors,” *Advanced devices & instrumentation*, 2021.

[12] R. Ramaswami, K. Sivarajan, and G. Sasaki, *Optical networks: a practical perspective*: Morgan Kaufmann, 2009.

[13] S. A. Mohammed, Y. Adamu, and L. Matthew, “Analysis of Dispersion Compensation in a Single Mode Optical Fiber Communication System,” *Int J Adv Acad Res*, vol. 5, no. 1, pp. 12-9, 2019.

[14] A. Czerwinski, and K. Czerwinska, "Statistical analysis of the photon loss in fiber-optic communication," *photonics*, vol. 9, no. 8, Art.no. 568, 2022.

[15] Y. Wang, K. Jiao, X. Liang, J. Jia, N. Li, S. Bai, X. Wang, Z. Zhao, Z. Liu, and P. Zhang, “Fabrication of mid-IR As-Se chalcogenide glass and fiber with low scattering loss,” *Journal of Lightwave Technology*, vol. 42, no. 9, pp. 3338-3345, 2024.

[16] P. Wang, J. Bei, N. Ahmed, A. K. L. Ng, and H. Ebendorff-Heidepriem, “Development of low-loss lead-germanate glass for mid-infrared fiber optics: I. Glass preparation optimization,” *Journal of the American Ceramic Society*, vol. 104, no. 2, pp. 860-876, 2021.

[17] F. A. Al-Bassam, J. H. Al-Asadi, W. Abdl-Daim, and G. Al-Dahash, “Studying the Attenuation Factors for SMF Optical Fiber,” *Journal of Babylon University/Pure and Applied Sciences*, vol. 20, no. 2, 2012.

[18] G. Keiser, "Fiber optic communication networks," *Fiber Optic Communications*, pp. 507-575: Springer, 2021.

[19] D. Melati, A. Melloni, and F. Morichetti, “Real photonic waveguides: guiding light through imperfections,” *Advances in Optics and Photonics*, vol. 6, no. 2, pp. 156-224, 2014.

[20] M. Ono, “Void engineering in silica glass for ultralow optical scattering loss,” *Journal of Lightwave Technology*, vol. 39, no. 16, pp. 5258-5262, 2021.

[21] K. Lathief, “Attenuation measurement in optical fiber communication,” *International Journals of Research Studies in Science, Engineering, and Technology (IJRSSET)*, vol. 4, no. 1, pp. 62-67, 2014.

[22] D. Arifler, and M. Guillaud, “Assessment of internal refractive index profile of stochastically inhomogeneous nuclear models via analysis of two-dimensional optical scattering patterns,” *Journal of biomedical optics*, vol. 26, no. 5, pp. 055001-055001, 2021.

[23] A. Volotka, A. Surzhykov, and S. Fritzsche, “Rayleigh scattering of linearly polarized light: Scenario of the complete experiment,” *Physical Review A*, vol. 102, no. 4, pp. 042814, 2020.

[24] S. f. Gao, Y. y. Wang, W. Ding, Y. f. Hong, and P. Wang, “Conquering the Rayleigh scattering limit of silica glass fiber at visible wavelengths with a hollow-core fiber approach,” *Laser & Photonics Reviews*, vol. 14, no. 1, pp. 1900241, 2020.

[25] W. Heitmann, and K.-F. Klein, “Infrared absorption of silica fibers,” *Journal of optical communications*, vol. 25, no. 3, pp. 106-109, 2004.

[26] G. P. Agrawal, *Fiber-optic communication systems*: John Wiley & Sons, 2012.

[27] V. A. Amorim, J. M. Maia, D. Viveiros, and P. Marques, “Loss mechanisms of optical waveguides inscribed in fused silica by

femtosecond laser direct writing," *Journal of Lightwave Technology*, vol. 37, no. 10, pp. 2240-2245, 2019.
[28] M. Gardies, M. Kemiche, D. Bucci, and E. Ghibaudo, "Interaction between spherical dielectric particles and surface integrated waveguides: a semi-analytical complex angle approach." pp. 230-235.
[29] G. Guerra, S. M. A. Mousavi, A. Taranta, E. N. Fokoua, M. Santagiustina, A. Galtarossa, F. Poletti, and L. Palmieri, "Unified coupled-mode theory for geometric and material perturbations in optical waveguides," *Journal of Lightwave Technology*, vol. 40, no. 14, pp. 4714-4727, 2022.
[30] J. L. Tsalamengas, "Oblique scattering from radially inhomogeneous bianisotropic cylindrical structures analyzed using a highly accurate Volterra integral equation approach," *IEEE Transactions on Antennas and Propagation*, vol. 69, no. 11, pp. 7811-7819, 2021.
[31] H. Kato, A. Nakamura, and S. Kinugasa, "Effects of angular dependency of particulate light scattering intensity on determination of samples with bimodal size distributions using dynamic light scattering methods," *Nanomaterials*, vol. 8, no. 9, pp. 708, 2018.
[32] P. Gautam, H. Moosmüller, J. B. Maughan, and C. M. Sorensen, "Light scattering from spherical and irregular particles over a wide angular range," *Aerosol Science and Technology*, vol. 58, no. 9, pp. 1053-1062, 2024.
[33] T. L. Singal, *Optical fiber communications: principles and applications*: Cambridge University Press, 2016.
[34] B. Yan, X. Zhang, and S. Guo, "Rapid ultraviolet curing of epoxy acrylate films with low refractive index and strong interfacial adhesion," *Reactive and Functional Polymers*, vol. 178, pp. 105356, 2022.
[35] J. M. Senior, and M. Y. Jamro, *Optical fiber communications: principles and practice*: Pearson Education, 2009.
[36] T. Ragin, A. Baranowska, M. Kochanowicz, J. Zmojda, P. Miluski, and D. Dorosz, "Study of mid-infrared emission and structural properties of heavy metal oxide glass and optical fibre co-doped with Ho3+/Yb3+ ions," *Materials*, vol. 12, no. 8, pp. 1238, 2019.
[37] G. Keiser, "Optical signal attenuation and dispersion," *Fiber Optic Communications*, pp. 93-145: Springer, 2021.
[38] G. M. Lo Piccolo, M. Cannas, and S. Agnello, "Intrinsic point defects in silica for fiber optics applications," *Materials*, vol. 14, no. 24, pp. 7682, 2021.
[39] M. E. Wandel, *Attenuation in silica-based optical fibers*: Technical University of Denmark, 2006.
[40] S. K. Bose, "Theoretical macrobending loss in single-mode transmission through a uniform index fiber-optic cable," *Optics Continuum*, vol. 1, no. 12, pp. 2521-2532, 2022.
[41] X. Qu, F. Ma, S. Zhao, L. Yang, Z. Wu, and B. Chen, "Analysis of the Influence of Macro-Bending Loss in Single-Mode Optical Fibers on Ofdr Signal Quality," 2025.
[42] A. Islam, and M. Ahmed, "Study of attenuation and bending losses in signal transmission over step index multimode PMMA fibers," *Int J Ambient Syst Appl*, vol. 8, 2020.
[43] X. Jin, and F. P. Payne, "Numerical investigation of microbending loss in optical fibres," *Journal of Lightwave Technology*, vol. 34, no. 4, pp. 1247-1253, 2016.
[44] L. N. Binh, "Optical fiber communication systems with Matlab and Simulink models," 2nd ed. *Boca Raton, FL, USA: CRC Press*, 2014.
[45] D. Bayuwati, and T. B. Waluyo, "Macro-bending loss of single-mode fiber beyond its operating wavelength," *TELKOMNIKA (Telecommunication Computing Electronics and Control)*, vol. 16, no. 1, pp. 142-150, 2018.
[46] A. Martins, A. M. Rocha, B. Neto, A. Teixeira, M. Facão, R. Nogueira, M. Lima, and P. Andre, "Modeling of bend losses in single-mode optical fibers," *Institutu de Telecomunicacoes, Portugal*, vol. 3, 2009.
[47] S. Sato, Y. Kawaguchi, H. Sakuma, T. Haruna, and T. Hasegawa, "Silica-core single-mode fiber with lowest loss of 0.1397 dB/km," *Journal of Lightwave Technology*, 2025.
[48] K. Tut Tahira, M. Omar Faruk, T. Ruma, T. Saha, and M. Rahman, "Analysis of fiber loss mechanisms in communication system to simulate different attenuation," *Journal of Engineering Research and Reports*, vol. 8, no. 1, pp. 1-15, 2019.
[49] H. Kanamori, "Transmission loss of optical fibers; achievements in half a century," *IEICE Transactions on Communications*, vol. 104, no. 8, pp. 922-933, 2021.
[50] M. Losada, A. López, and J. Mateo, "Attenuation and diffusion produced by small-radius curvatures in POFs," *Optics Express*, vol. 24, no. 14, pp. 15710-15720, 2016.
[51] A. M. Jassim, H. A. Yasser, and H. K. Muhammad, "Numerical Study of Bending Losses in Optical Fibers with Arbitrary Profile Index." p. 032081.